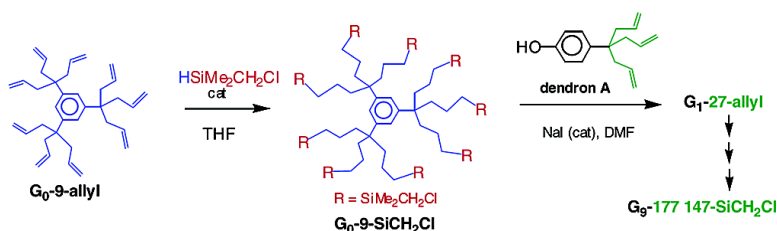


Construction of Giant Dendrimers Using a Tripodal Building Block

Jaime Ruiz, Gustavo Lafuente, Sylvia Marcen, Catia Ornelas,
 Sylvain Lazare, Eric Cloutet, Jean-Claude Blais, and Didier Astruc

J. Am. Chem. Soc., **2003**, 125 (24), 7250-7257 • DOI: 10.1021/ja021147o • Publication Date (Web): 21 May 2003

Downloaded from <http://pubs.acs.org> on March 29, 2009



More About This Article

Additional resources and features associated with this article are available within the HTML version:

- Supporting Information
- Links to the 14 articles that cite this article, as of the time of this article download
- Access to high resolution figures
- Links to articles and content related to this article
- Copyright permission to reproduce figures and/or text from this article

[View the Full Text HTML](#)

Construction of Giant Dendrimers Using a Tripodal Building Block

Jaime Ruiz,[†] Gustavo Lafuente,[†] Sylvia Marcen,[†] Catia Ornelas,[†] Sylvain Lazare,[‡] Eric Cloutet,[§] Jean-Claude Blais,[⊥] and Didier Astruc^{*,†}

Contribution from the Laboratoire de Chimie Organique et Organométallique, UMR CNRS No. 5802, Laboratoire de Physico-Chimie Moléculaire, UMR CNRS 5803, Laboratoire de Chimie des Polymères Organiques, UMR CNRS 5629, Université Bordeaux I, 33405 Talence Cedex, France, and Laboratoire de Chimie Structurale Organique et Biologique, UMR CNRS No. 7613, Université Paris VI, 4 Place Jussieu, 75252 Paris, France

Received September 4, 2002; E-mail: d.astruc@lcoo.u-bordeaux.fr

Abstract: Giant pentane-soluble organo-silicon dendrimers have been synthesized using a triallylphenol brick according to a new divergent construction that uses a hydrosilylation–nucleophilic substitution sequence up to the ninth generation (G_9). All the reactions were monitored by ^1H , ^{13}C , and ^{29}Si NMR until G_9 , indicating that they were clean at the NMR accuracy until this last generation. MALDI TOF mass spectra were recorded for G_1 to G_4 and show the nature and amounts of defects that are intrinsic to the divergent construction. This technique and SEC (recorded up to G_5) confirm the monodispersity (1.00 to 1.02) from G_1 to G_5 . HRTEM and AFM images recorded for the high generations disclose the expected smooth dendrimer size progression and the globular shape. At G_9 , the theoretical number of termini (TNT) is 177 407 branches (abbreviation: G_9 -177 047). It is estimated that more than 10^5 terminal branches are actually present in the G_9 dendrimer, far beyond the De Gennes “dense-packing” limit (6000 branches), and it is believed that the branch termini turn inside the dendrimer toward the core. This is corroborated by lower reaction rates and yields for the highest generation numbers presumably due to intradendritic reactions. It is probable that the dendritic construction is limited by the density of branches inside the dendrimer, i.e., far beyond the dense-packing limit.

Introduction

Dendrimers have numerous potential applications in biology, catalysis, and materials science.^{1–8} This field of molecular science is now well spread, yet only very few syntheses and characterizations of very large dendrimers have been reported. The largest dendrimers whose characterizations have been

published^{9–11} have total numbers of termini (TNT) up to about 3000. One report appeared for large dendrimers with up to more than 2×10^6 branches, but these dendrimers were not characterized by spectroscopy, mass spectra, or microscopy beyond the first generation, and their construction might have been marred by cross-linking.¹² Other large dendrimer constructions were not larger than the dense-packing limit.¹³ Two groups have reported that dendrimers terminated by amino groups become insoluble when the TNT reaches the dense-packing limit (TNT: 3072⁹ and 6144¹¹). These observations seemingly confirm De Gennes’ dense-packing theory¹³ set for PAMAM dendrimers according to which the steric congestion occurring at the dendritic surface inhibits further regular dendrimer

[†] LCOO, Université Bordeaux I.

[‡] LPCM, Université Bordeaux I.

[§] LPCO, Université Bordeaux I.

[⊥] LCSOB, Université Paris VI.

- (1) (a) Tomalia, D. A.; Taylor, A. N.; Goddard, W. A., III. *Angew. Chem. Int. Ed. Engl.* **1990**, *29*, 138–175. (b) Fréchet, J. M. J. *Science*, **1994**, *263*, 1710–1715. (c) Ardoin, N.; Astruc, D. *Bull. Soc. Chim. Fr.* **1995**, *132*, 875–909.
- (2) (a) Newkome, G. R.; Moorefield, C. N.; Vögtle, F. *Dendrimers and Dendrons: Concepts, Syntheses and Applications*; VCH: Weinheim, 2001. (b) *Advances in Dendritic Molecules*; Newkome, G., Ed.; JAI: Greenwich, CT, Vols. 1–5, 1994–1998 and 2002. (c) *Dendrimers, Topics in Current Chemistry*; Vögtle, F., Ed.; Springer-Verlag: Berlin, Vol. 1, 1997; and Vol 2, 2000. (d) *Dendrimers and Other Dendritic Polymers*; Tomalia, D., Fréchet, J. M. J., Eds.; Wiley-VCH: New York, 2002.
- (3) Zeng, F.; Zimmerman, S. C. *Chem. Rev.* **1997**, *97*, 1681–1712.
- (4) Matthews, O. A.; Shipway, A. N.; Stoddart, J. F. *Prog. Polym. Sci.* **1998**, *23*, 1–56.
- (5) Venturi, M.; Serroni, S.; Juris, A.; Campagna, S.; Balzani, V. In *Dendrimers, Topics in Current Chemistry*; Vögtle, F., Ed.; Springer-Verlag: Berlin, 1998; Vol. 197, pp 193–228.
- (6) (a) Bosman, A. W.; Janssen, H. M.; Meijer, E. W. *Chem. Rev.* **1999**, *99*, 1665–1688. (b) Sijbesma, R. P.; Meijer, E. W. *Curr. Opin. Int. Sci.* **1999**, *4*, 24–34. (c) Weener, J.-W.; Baars, M. W. P. L.; Meijer, E. W. In ref 2d, pp 387–424. (d) Bosman, A. W.; Bruining, M. J.; Kooijman; Spek, A. L.; Janssen, R. A. J.; Meijer, E. W. *J. Am. Chem. Soc.* **1998**, *120*, 5547–8548.

- (7) (a) Hecht, S.; Fréchet, J. M. J. *Angew. Chem., Int. Ed.* **2001**, *40*, 74–91. (b) Fréchet, J. M. J. *Chem. Rev.* **2001**, *101*, 3819–3867. (c) Aliphatic ester dendrimers up to 30 711 Da and 192 masked hydroxyl groups (in six generations) have recently been conveniently prepared in high yield and purity: Ihre, H.; Padilla De Jesús, O. L.; Fréchet, J. M. J. *J. Am. Chem. Soc.* **2001**, *123*, 5908–5917.
- (8) Crooks, R. M.; Zhao, M.; Sun, L.; Chechik, V.; Yeung, L. K. *Acc. Chem. Res.* **2001**, *34*, 181–190.
- (9) Tomalia, D. A.; Baker, H.; Dewald, J. R.; Hall, M.; Kallós, G.; Martin, S.; Roeck, J.; Ryder, J.; Smith, P. *Macromolecules* **1986**, *19*, 2466–2470.
- (10) van der Made, A. W.; van Leeuwen, P. W. N. M.; de Wilde, J. C.; Brandes, R. A. C. *Adv. Mater.* **1993**, *5*, 466–468.
- (11) Caminade, A. M.; Majoral, J. P. In *Dendrimers, Topics in Current Chemistry*; Vögtle, F., Ed.; Springer: Berlin, 1998; pp 79–124.
- (12) Sourmies, F.; Crasnier, F.; Graffeuil, M.; Faucher, J.-P.; Lahana, R.; Labarre, M. C.; Labarre, J.-F. *Angew. Chem., Int. Ed. Engl.* **1995**, *34*, 578–581.
- (13) De Gennes, P.-G.; Hervet, H. *J. Phys. Lett.* **1983**, *44*, 351–360.

construction, the space A_Z available on the dendrimer surface for each terminal group at the dendrimer periphery being given by

$$A_Z = A_D/N_Z \propto r^2/N_c N_b G \quad (1)$$

in which A_D is the total surface of the periphery, N_Z the number of termini, r the radius of the dendrimer sphere, N_c the number of core branches, N_b the multiplication number at each focal point, and G the generation number. De Gennes' dense-packing (limit) generation G_1 follows:

$$G_1 = a(\ln P + b) \quad (2)$$

where P is the length of the branch-cell segment, and a and b are parameters that depend on the type of dendrimer ($a = 2.88$ and $b = 1.5$ for Tomalia's PAMAM dendrimers^{1,9}). This theory seemingly holds well when the branches are terminated by groups that give hydrogen bonding¹ or bear charges,^{2,3,6} large groups,¹⁻³ or perfluoro groups causing monomer–monomer attraction¹⁴ or if the dendrimer has rigid tethers. Besides these cases, it remained essential, however, to clarify whether the dense-packing limit was more generally valid. Other calculations have indeed proposed that the branches turn toward the inside of the dendrimer and that, consequently, the density is larger inside the dendrimer near the core than at the surface.¹⁵⁻¹⁷ Viscosimetry,¹⁸ solid state NMR,¹⁹ ¹³C and ²H NMR relaxation times,²⁰ and fluorescence depolarization²¹ studies have also suggested that the branches are partly backfolded toward the inside of the dendrimer.^{6d}

We report here a dendrimer construction extending beyond the dense-packing limit that is supported *inter alia* by ¹H, ¹³C, and ²⁹Si NMR spectra recorded after each reaction, indicating that these reactions are clean within the NMR accuracy.

Results

The dendritic core and the brick used to construct the dendrimers were synthesized under very mild conditions using high-yield CpFe⁺-induced perallylation of simple methyl or polymethyl aromatics. Among these known reactions, we have chosen the CpFe⁺-induced nona-allylation of mesitylene for the synthesis of a nona-allyl core²² and the CpFe⁺-induced triallylation of *p*-ethoxytoluene that also proceeds with CpFe⁺-induced aryl ether cleavage and yields the triallylphenol brick. This simple tripodal compound is now accessible in 60% yield from its easily available precursor [FeCp(η^6 -*p*-Cl-C₆H₄OEt)] [PF₆].²² We have already reported a tentative divergent dendrimer synthesis using these units.²² It was based on the hydroboration

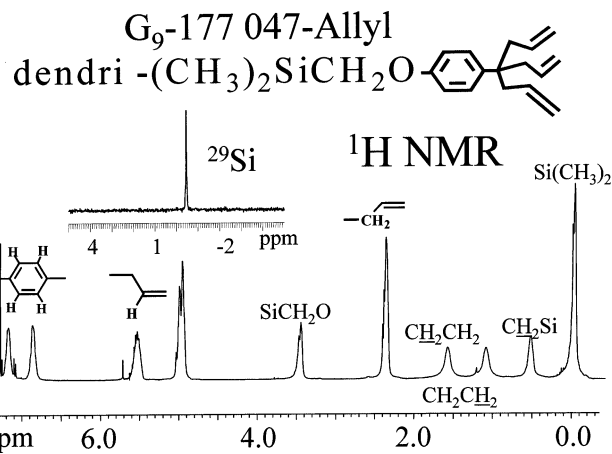


Figure 1. 400 MHz ¹H and 100 MHz ²⁹Si NMR spectra of the G₉-177 047-allyl dendrimer, which very clearly show the signals of the surface phenoxy, allyl, and methylene protons and the single ²⁹Si peak.

of the polyallyl core, synthesis of the mesylate, and then nucleophilic substitution of the latter by the phenolate. The yield of the second-generation dendrimer was low because of the steric limit due to the bulk of the large borane groups, which prevented an efficient construction of high generations.

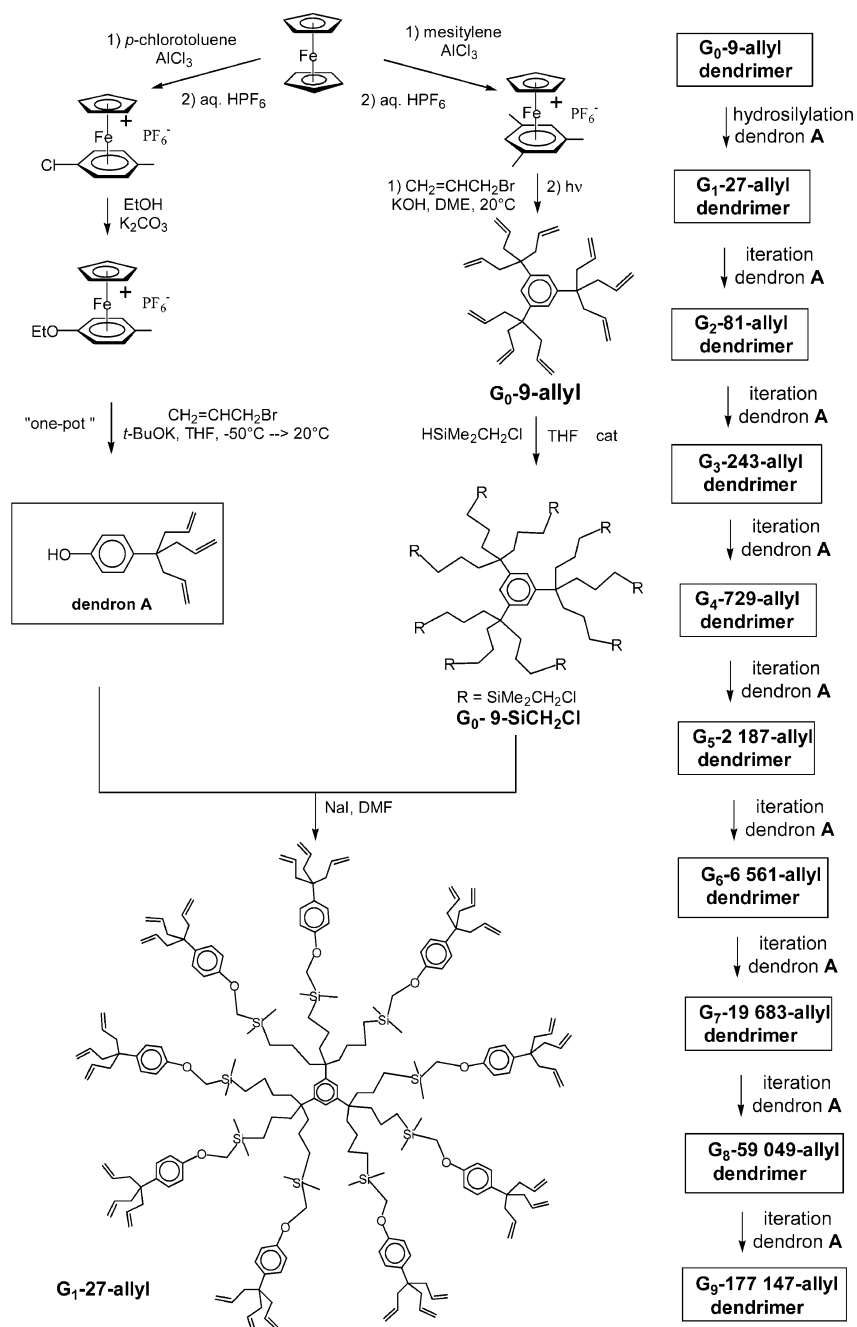
In the present work (see Scheme 1), tethers longer than in the previous dendrimers have been designed, which circumvents this problem. The strategy is based first on the hydrosilylation of the polyolefin core catalyzed by the Karstedt catalyst in ether using dimethylchloromethylsilane, a reagent already successfully used by Seyferth²³ for dendrimer synthesis. The second reaction of the sequence for each generation is the nucleophilic substitution of the terminal chloride by the phenolate group of the triallylphenol catalyzed by sodium iodide in DMF. At each generation, the reaction mixture is passed rapidly through a short column of silica gel after the hydrosilylation in order to remove the catalyst, then the solvent is removed and the residue is submitted without further purification to the second reaction of the sequence. Indeed, the hydrosilylation is virtually quantitative without isomerization according to the accuracy provided by ¹H NMR. After the second reaction, the solvent is removed under vacuum, the residue is dissolved in the minimum of methylene chloride, and the dendrimer is precipitated by addition of excess methanol. Then, the gum is dissolved in methylene chloride and submitted to flash chromatography on silica gel, yielding an off-white gum after removing the solvent. Although this procedure lowers the yield, the spectroscopic and analytical data are well optimized in this way.

The dendritic construction could be repeated until the ninth generation. Figures 1 and 2 show the ¹H and ²⁹Si NMR spectra of the dendrimers G₉-177 047 and those of its hydrosilylation product, respectively. The yields were relatively good for the first generations, then progressively decreased (see Tables 1 and 2). At the ninth generation, the yield of purified product became low (8%). The elemental analyses were quite satisfactory until G₄-2187, then the carbon content found became deficient for the higher generation numbers (by 1.3–3.4%), implying that impurities were encapsulated inside the dendrimers.

The purity was monitored at each generation by ¹H and ²⁹Si NMR, and the spectra were always quite clean, showing only the groups present at the periphery of the dendrimers (two last

- (14) Percec, V.; Johansson, G.; Ungar, G.; Zhou, J. P. *J. Am. Chem. Soc.* **1996**, *118*, 9855–9866.
 (15) Lescanec, R. L.; Muthukumar, M. *Macromolecules* **1990**, *23*, 2280–2288.
 (16) (a) Mansfield, M. L.; Klushin, L. I. *Macromolecules* **1993**, *26*, 4262–4268. (b) Boris, D.; Rubinstein, M. *Macromolecules* **1996**, *29*, 7251–7260.
 (17) Naidoo, K. J.; Hughes, S. J.; Moss, J. R. *Macromolecules* **1999**, *32*, 331–341.
 (18) Mourey, T. H.; Turner, S. R.; Rubinstein, M.; Fréchet, J. M. J.; Hawker, C. J.; Wooley, K. L. *Macromolecules* **1992**, *25*, 2401–2406.
 (19) Wooley, K. L.; Klug, C. A.; Tasaki, K.; Schaefer, J. J. *J. Am. Chem. Soc.* **1997**, *119*, 53–58.
 (20) Meltzer, A. D.; Tirrell, D. A.; Jones, A. A.; Inglefield, P. T.; Hedstrand, D. M.; Tomalia, D. A. *Macromolecules* **1992**, *25*, 4549–4552.
 (21) De Backer, S.; Prinzie, Y.; Verheijen, W.; Smet, M.; Desmedt, K.; Dehaen, W.; De Schryver, F. C. *J. Phys. Chem. A* **1998**, *102*, 5451–5455.
 (22) Sartor, V.; Djakovitch, L.; Fillaut, J.-L.; Moulines, F.; Neveu, F.; Marvaud, V.; Guittard, J.; Blais, J.-C.; Astruc, D. *J. Am. Chem. Soc.* **1999**, *121*, 2929–2930.

- (23) Krsda, S. W.; Seyferth, D. *J. Am. Chem. Soc.* **1998**, *120*, 3604–3612.

Scheme 1. Overall Dendrimer Construction Starting from Ferrocene^a

^a The nona-allyl core synthesized by CpFe⁺-induced nona-allylation of mesitylene followed by decomplexation using visible light (right column) can be considered as G₀ and thus the 27-allyl derivative, represented below, as G₁ (abbreviation: G₁-27).

generations, the other generations having too few protons to be observable). From one generation to the next, these spectra remained essentially the same until the ninth generation (Figures 1 and 2). The hydrosilylation reactions were monitored in ¹H NMR by the disappearance of the allyl signals at 2.4, 5.0, and 5.5 ppm and the appearance of the sharp singlet corresponding to SiCH₂Cl at 2 ppm. The nucleophilic substitutions by the triallylphenate were monitored by the disappearance of this singlet and the increase of the SiCH₂O signal at 3.5 ppm and of the phenol signals at 6.9 and 7.2 ppm. The only side reaction that would also lead to a shift from the SiCH₂Cl or SiCH₂I signal to a SiCH₂OR signal different from that with R = triallylphenol would be that with adventitious water, which would lead to a

SiCH₂OH branch (R = H). This side reaction can be discarded as follows, however. The mass spectra of the dendrimers G₁-27 and G₂-81-allyl do show that such a branch is not formed. If this side reaction would occur for the high generations, the intensity of the signals of the phenol group versus that of the SiCH₂OH signal would be weaker than the theoretical one, which is not observed. Finally, the zeroth-generation nona-alcohol dendrimer G₀-9-SiCH₂OH has been synthesized, and its SiCH₂OH methylene signal appears at 3.27 ppm.²⁴ Mixing

(24) In accord with our data, a nearly identical ¹H NMR chemical shift in CDCl₃ (3.22 ppm) for a compound also containing the -SiCH₂OH group was recently reported: Tacke, R.; Handmann, V. I. *Organometallics* **2002**, *21*, 2619–2625.

Table 1. Characteristics of the Nine Generations of Polyallyl Dendrimers (G₁-27 to G₉-177 147)

Generation ^a	Number of allyl branches ^b	Diameter, nm full extension (molecular model) ^c	Height by AFM (± 5%) ^d	Molecular weight (molecular peak ^e) Da	Polydispersity by SEC ^f
0	9	1.25 nm		481 (X-ray structure)	
1	27	2.86 nm (2.3 nm)	M	3 185 (3 185)	
2	81	4.60 nm (4.0 nm)		11 299 (11 300)	1.01
3	243	6.32 nm (5.5 nm)		35 660 (35 640)	1.01
4	729	8.06 nm	6 nm	108 664 (traces 108 432)	1.01
5	2 187	9.80 nm	8.5 nm	327 735	1.00
6	6 561	11.54 nm	B	984 948	
7	19 683	13.28 nm		2 956 588	
8	59 049	15.02 nm		8 871 506	
9	177 147	16.76 nm	26 nm	26 616 261	

^a See Scheme 1 and Figures 3 and 4 for G₁-G₃. ^b Theoretical branch numbers. ^c See text and Figure 3. ^d M: monolayer; B: flattened bilayer. ^e Molecular peak found by MALDI TOF mass spectrometry. ^f Size-exclusion chromatography, see Figure 5.

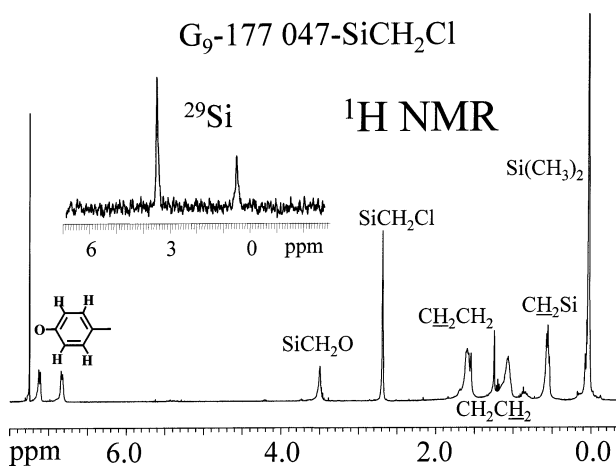


Figure 2. 400 MHz ¹H and 100 MHz ²⁹Si NMR spectra of G₉-177 147-SiCH₂Cl resulting from the catalyzed hydrosilylation of G₉-177 147-allyl (see text). See the HRTEM of the iodo analogue in Figure 7.

Table 2. Yields (% and mass) Obtained from Generation to Generation and Elemental Analyses (H and C) of the Dendrimers

	anal. calcd		anal. found		yield from G _{n-1}	
					%	mass (g)
G ₁ -27-allyl	9.49	78.05	9.50	78.25	73	0.480
G ₂ -81-allyl	9.42	76.53	9.22	76.47	58	0.890
G ₃ -243-allyl	9.40	76.12	9.60	76.47	54	1.530
G ₄ -729-allyl	9.39	76.00	9.38	75.42	48	2.240
G ₅ -2187-allyl	9.39	75.96	9.39	74.69	35	2.360
G ₆ -6561-allyl	9.39	75.96	9.66	73.47	28	1.980
G ₇ -19 683-allyl	9.39	75.94	10.04	72.62	27	1.610
G ₈ -59 049-allyl	9.39	75.94	9.50	73.28	23	1.110
G ₉ -177 147-allyl					8	0.270

^a In a series of experiments, all the analytical and spectroscopic data were collected (see Experimental Section). In another series, the whole sample (masses in the table) was used for the synthesis of the following generation after checking completion of the reactions by ¹H NMR and extensive purification after each reaction as indicated in the text.

it with G₂-81-allyl clearly shows both distinct methylene signals due to the two compounds (see the NMR spectra in the Supporting Information). An organic impurity sometimes observed by NMR for the high generations is an alkane residue

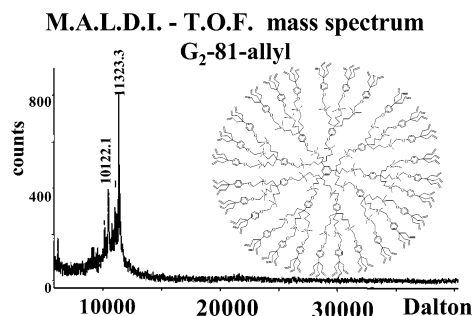


Figure 3. MALDI TOF mass spectrum of G₂-81-allyl-dendrimer. The major peak is the molecular peak (M = 11 299; [M + Na]⁺ at *m/z* 11 322). The minor peak at 10 422 represents the same dendrimer in which one triallylphenol unit is missing, possibly because of the isomerization of a double bond during the catalyzed hydrosilylation reaction (see text).

(impurity coming from the silica gel). It could be almost completely removed by successive reprecipitation, but a very minor part remained trapped inside the dendrimers.

The ²⁹Si spectra were particularly simple. The hydrosilylation gave a compound that showed two ²⁹Si NMR signals at 0.40 and 3.8 ppm, and the polyolefin dendrimers showed only one signal at 0.40 ppm. The dendrimers remained pentane soluble until the ninth generation, and the ¹H and ²⁹Si NMR spectra are shown in Figure 1. Although the impurities attached to the dendrimers cannot be seen within the NMR accuracy (<5%), the difference between the theoretical number of branches and the actual number increases at each generation as in every divergent construction, and this is well observed by MALDI TOF mass spectroscopy (Figure 3 and Supporting Information). For instance, the spectrum of G₂-81 in Figure 3 shows the dominant molecular peak at 11 323 Da, but also a small side peak showing the lack of one tripod unit (26 tripods instead of 27). This indicates that the nucleophilic substitution worked with a conversion of only about 99%. That of the next generation (243 branches, see a drawing and molecular modeling in Figure 4) shows the molecular peak at 35 640 Da, but it is now a minor peak, whereas the impurities dominate at lower mass. Thus, the conversion is not quantitative and might thus decrease as the generation number increases, although the defects are not seen

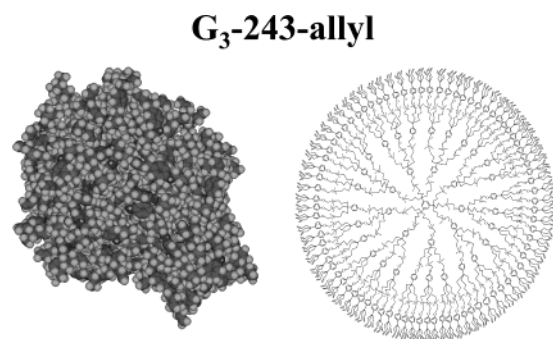


Figure 4. G₃-243-allyl dendrimer (right, see Scheme 1 for the synthesis) and its molecular model (left). The molecular peak is observed in its MALDI TOF mass spectrum, and the polydispersity value is 1.02 (see also Figure 5 and Table 1 for SEC and polydispersity data).

Size exclusion chromatography dendri - allyl (G₁- G₅)

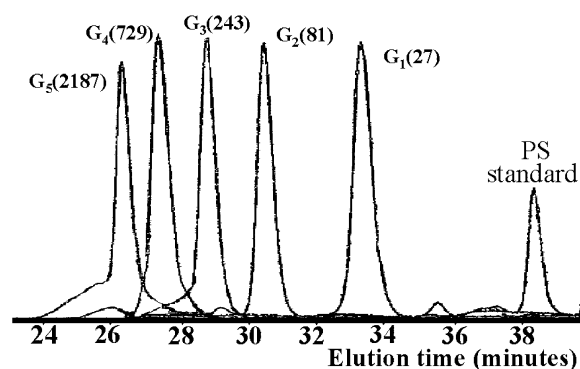


Figure 5. Size exclusion chromatograms (SEC) of all the dendrimers from G₁ to G₅. The generations and numbers of allyl groups are noted above each chromatogram on the figure. The polydispersities obtained from these SECs have values between 1.00 and 1.02 up to G₅. Above this generation, the SEC could not be obtained so far because the dendrimer size overtakes 10⁶ um and the globular shape requires much larger pores than for linear polymers (SEC for dendrimers overtaking 10⁶ um have, to our knowledge, not yet been recorded). The presence of the minor bands at high masses is probably due to aggregates of dendrimers whose formation is all the more important as the dendritic size is larger, as shown by AFM (see Figure 8).

within the NMR accuracy. For G₄-729, the broad spectrum vanished near the region of the molar mass at 108 664 Da. The size exclusion chromatography (SEC) could be recorded for the five first generations (Figure 5).

MALDI TOF and SEC yielded polydispersity data of 1.00–1.02 for G₃-243, G₄-729, and G₅-2 187 (Table 1). For G₄-729 (as for the others), the transmission electron microscopy (TEM) does not give any image because the dendrimer contains only light atoms. Vaporization of osmium oxide onto the sample, however, allowed the observation of the individual dendrimers using this technique, because of the formation of glycolate metalocycles including the heavy osmium atoms covalently bound at the periphery of the dendrimer (Figure 6). **Caution:** osmium oxide is toxic and must be handled under a well-ventilated hood. The TEM could be recorded for G₉ after hydrosilylation with dimethylchloromethylsilane followed by exchange of Cl by I with NaI in refluxing butanone. This gives a TEM image whose average diameter is 13 nm (Figure 6).

Finally, atomic force microscopy (AFM) was a valuable tool to examine the polyallyl dendrimers for all the generations, since the height of the dendrimers is easily measurable,

HRTEM G₄-729-allyl

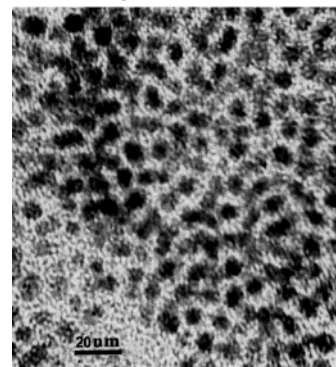


Figure 6. HRTEM picture of G₄-729 coated with osmium oxide vapor and recorded on amorphous graphite support. Osmium oxide forms a five-membered glycolate metalocycle by addition of the terminal double bonds of the branches onto oxo ligands³⁷ (the proportion of reacted terminal double bonds is unknown).

HRTEM G₉-177 047-SiCH₂I

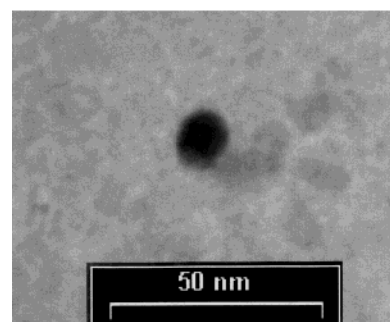


Figure 7. HRTEM picture of G₉-177 047-SiCH₂I recorded on amorphous graphite support showing the globular shape with a diameter of 13 nm (compare Table 1 and Figure 8) lower than that calculated (16.7 nm) for tethers with maximum extension. See the ¹H and ²⁹Si NMR spectra of the chloro analogue of this compound in Figure 2.

as shown in Figure 8 for G₉. The images show large aggregates corresponding to more than 100 dendrimers. The remarkably smooth progression of the heights of the samples with increasing generation numbers shows monolayers for the first five generations and double layers for the last four generations. Flattening^{25–27} and aggregation^{28–30} of dendrimers recorded by AFM have already been observed in other cases. The heights of the monolayers are slightly lower than those calculated until G₅, whereas the height corresponds to a double layer of even more flattened dendrimers from G₆ to G₉ (Table 1 and Figure 8). Although the increase of the number of layers (from mono to bi) with generation is not too surprising, a precise understand-

- (25) Hierleman, A.; Campbell, J. K.; Crooks, A. M.; Rico, A. J. *J. Am. Chem. Soc.* **1998**, *120*, 5323–5324.
- (26) Li, J.; Swanson, D. R.; Qin, D.; Brothers, H. M.; Piehler, L. T.; Tomalia, D.; Meier, J. *Langmuir* **1999**, *15*, 7347–7350.
- (27) Tsukruk, V. V.; Rinderspacher, F.; Bliznyuk, V. N. *Langmuir* **1997**, *13*, 2171–2176.
- (28) Sheiko, S. S.; Gauthier, M.; Möller, M. *Macromolecules* **1997**, *30*, 2343–2349.
- (29) Díaz, D. J.; Storrer, G. D.; Bernhard, S.; Takada, K.; Abruña, H. D. *Langmuir* **1999**, *15*, 7351–7354.
- (30) Sano, M.; Okamura, J.; Ikeda, A.; Shinkai, S. A. *Langmuir* **2001**, *17*, 1807–1810.

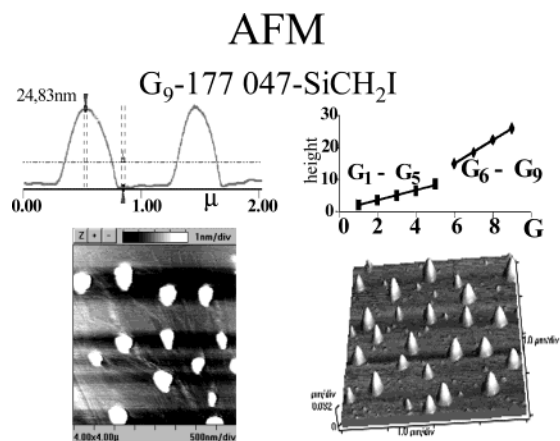


Figure 8. AFM images of G₉-177 047-SiCH₂I on graphite HOPG support shown in two dimensions (left) and three dimensions (right). The diameters are 100 nm on average, and the height is 25 nm (top), indicating the aggregation of about 100 dendrimers in a double layer (compare Table 1 and Figure 5). AFM was operated in the tapping mode with a resonance frequency of around 200 MHz. The tip has a radius of 10 nm. The top right graph shows the progression of the height of the polyallyl dendrimers determined by AFM from the first to the ninth generation (G₁–G₉) involving monolayers from G₁ to G₅ and bilayers from G₆ to G₉ (see also Table 1).

ing of why double layers form for the last generations is not obvious at present, and more investigations are called for in order to fully rationalize these events.

Discussion

The present dendrimer construction provides a rapid increase of the number of branches, because this number is multiplied by 3 at each generation. This is a 1 → 3 C-branched connectivity,^{2a} the first example of which was reported by Newkome in his seminal 1985 article with a 27-arborol.³¹ For instance, this strategy allows the rapid and easy synthesis of the dendrimer G₄-729 with a total yield of 11% from G₀-9 (this yield includes purification after each reaction), which corresponds to a 10-fold increase of mass from of G₀-9 (see Table 2). Previous divergent dendrimer syntheses required a high number of generations to reach such a number of branches, because their connectivity was usually only two.^{1a,2a,6a,7d} The divergent construction is marred by the well-known problem of the defects. Yet, the synthesis of G₂-81, which is almost pure, in 42% total yield and 9-fold mass increase from G₀-9 (including purification after each reaction) sets this synthesis among the successful ones along with only a few others.^{1a,2a,4,6a,7c} The level of defects is such that they are not observed by NMR and are thus restricted to a low additional amount at each generation.

NMR is an excellent technique showing the construction step by step with at least 95% conversion (worst NMR accuracy), and the TEM and AFM indicate the globular shape and the regular macroscopic progression of the size with the increase of generation number. What is missing, however, is information of the actual number of branches (or defects) for the large dendrimers and the polydispersities of the last generations. For instance, with only 99% conversion of a pure G₂ dendrimer, almost none of the pure G₃ dendrimer should be obtained even if the polydispersity is 1.00 (compare with the presence of a minor molecular peak for the 243-allyl dendrimer). It is also especially difficult to speculate on the numbers of branches for

the high generation numbers since the conversion may decrease as the number of generations increases. If the conversions are 95%, about 12 000 branches are missing in the ninth generation; thus more than 10⁵ branches must be present in this giant dendrimer of 13 nm diameter. This number is far beyond De Gennes' dense-packing limit.¹³ First, it should be noted that this limit deals with theoretically pure dendrimers, and we know that we are not in this case because of the defects. The De Gennes theory states that one cannot construct the dendrimer in a divergent way without defects, due to lack of space at the periphery. Thus, it views the branch termini as being located at the periphery of the dendrimers. Dendrimers become insoluble when the steric saturation of the termini is reached at the periphery, and indeed such insolubility has been sometimes attributed to the De Gennes dense-packing limit.¹³ Dendrimer chemists encounter this problem when the termini of the branches are bulky. On the other hand, when the branch termini are flexible and nonbulky, these termini can turn inside the dendrimers and fill the internal cavities that are apparent in a static model. From calculations, it has been suggested that the proportion of branch termini that turn inside the dendrimer diminishes as the termini become bulkier.¹⁷ The defects present in our dendrimers are in too small number (even in the worse case) to state that the termini remain at the periphery for the highest generation numbers. On the contrary, for higher generations, the proportion of termini turned inside the dendrimer must dramatically increase with the generation number.

The maximum number of terminal methylene groups located at the dendrimer surface can be estimated using De Gennes' eq 1. By comparing the calculated length of the tether at full extension and the diameter of the molecular model of G₃ in Figure 2, the diameter indicated by this model is about 11.5% shorter than that corresponding to full extension. If one extrapolates this slight correction, the diameter of the G₆ dendrimer is estimated to be about 10 nm, corresponding to a surface of 314 nm² if it is considered to be spherical. The van der Waals surface of a terminal olefinic methylene group is 0.09 nm², yielding a maximum of about 3500 surface methylene groups, i.e., about half the total number. This maximum increases with the generation number and reaches about 6000 for the G₉ dendrimer, i.e., only about 6% of the terminal groups actually present in this dendrimer. In a dynamic view, one could say that the termini spend only 6% of their time in the periphery and 94% inside the dendrimer.

We have noted that the reaction times required to reach completion increase with the generation number. The reaction yields concomitantly decrease because prolonged heating in DMF at 80 °C causes some decomposition whose (unknown) products are removed during the chromatographic purification. Another potential reason for enhanced decomposition when the generation number increases may eventually also be that the density of branches in the dendrimer favors interbranch collisions. Thus, the dendrimer constructions are not actually limited, in the general case (absence of rigidity, large terminal groups, or H-bonding among these groups), by the bulk at the periphery that would be due to the presence of all the termini at the periphery. It is also probable that the termini turn toward the core for generation numbers well below that corresponding to the dense-packing limit, as suggested previously.^{15–21} The dense-packing limit provokes a lowering of the reaction rates, however,

(31) Newkome, G. R.; Yao, Z.; Baker, G. R.; Gupta, V. K. *J. Org. Chem.* **1985**, *50*, 2003–2004.

due to the fact that the reactions of the termini have to take place to a large extent inside the dendrimers beyond this limit. On the other hand, the branch density inside the dendrimer volume limits this construction, but at a much higher number of generations than that corresponding to the dense-packing limit, because the branches mostly turn inside toward the core. Indeed, the reaction yields decrease when the generation number increases and dramatically drop at G_9 .

Conclusion

A new family of large dendrimers has been synthesized using a tripodal branching unit that multiplies the branch number by 3 at each generation up to a diameter of 13 nm, as shown by TEM and AFM, and branch numbers superior to 10^5 at the ninth generation. The TEM shows the globular shape, and the AFM illustrates the smooth size progression. The two reactions of the sequence were monitored by NMR and shown to be clean on the NMR accuracy, which indicates that the percentage of defects is small at each generation. The nature and amount of defects could be identified by MALDI TOF mass spectrometry for the first generations. The very large dendrimer sizes obtained and the small proportions of defects show that the construction proceeds far beyond the dense-packing limit. We speculate that, for the highest generation numbers, the small flexible branch termini turn inside toward the dendritic core to a large extent, all the more so as the generation number is higher. The construction is limited by the density inside the dendrimer rather than by the bulk of the termini at the periphery. Thus, this limit is pushed far beyond the “dense-packing limit”. This is corroborated by low reaction rates and yields for the highest generation numbers for which the reactions presumably take place to a large extent within the dendrimer. Finally, the feasibility of the synthesis of giant dendrimers far beyond the dense-packing limit opens a new scope of supramolecular chemistry³² involving dendritic structures.

Experimental Section

The precursor complexes $[\text{FeCp}(\eta^6\text{-arene})][\text{PF}_6]$,³³ the nona-allyl core,^{22,35} and the dendron **A**^{22,34} are synthesized according to literature (see ref 35 for the X-ray crystal structure of the nona-allyl core).

First Reaction of the Dendritic Sequence: Hydrosilylation of the Polyallyl Dendrimers. Example of the Nona-allyl Core G_0 . To 0.500 g (1.04 mmol) of the nona-allyl core G_0 in a Schlenk flask is added 20 mL of dry ether, then, in a Vacuum-Atmosphere Corp. dry lab, 12 drops of a commercial xylene solution (2%) of the Karstedt catalyst bis(divinyltetramethyldisiloxane)platinum (see ref 36³⁷) and 1.520 g (13.94 mmol) of dimethylchloromethylsilane are added. The reaction mixture is allowed to stir under argon for 3 days at room temperature, then filtered over a short column of silica in order to remove the catalyst. The solvent and excess silane are removed under vacuum, and a yellow

oil is obtained (1.500 g; 98%). See the ^1H and ^{29}Si NMR in Figures 1 and 2 (the spectra are similar for all the generations, except that, in addition, the three arene core protons are observed as a singlet at 6.99 ppm for only G_0 and G_1 in the ^1H NMR spectra). Also, alkane signals are observed with variable intensities. It comes from the xylene solvent of the Karstedt catalyst and can be partly removed, but not completely, from the dendrimer by reprecipitation from a dichloromethane solution using methanol. ^1H NMR (CDCl_3 , 300 MHz, δ_{ppm} vs TMS): 6.96 (Ar, s), 2.73 (CH_2Cl , s), 1.60 ($\text{CH}_2\text{CH}_2\text{CH}_2\text{Si}$, m), 1.09 ($\text{CH}_2\text{CH}_2\text{CH}_2\text{Si}$, m), 0.60 ($\text{CH}_2\text{CH}_2\text{CH}_2\text{Si}$, t), 0.06 (SiMe_2 , s). ^{29}Si NMR (CDCl_3 , 59.6 MHz, δ_{ppm} vs TMS): 3.85. The ^{29}Si NMR of the higher generations $G_n\text{-SiCH}_2\text{Cl}$ shows two peaks: 3.8 ppm (SiCH_2Cl) and 0.73 ppm (SiCH_2O). ^{13}C NMR (100.6 MHz, δ_{ppm} vs. TMS): 145.6 (substituted arene C), 121.4 (arene CH). These core arene C atoms are observable only for $G_0\text{-SiCH}_2\text{Cl}$ and $G_1\text{-SiCH}_2\text{Cl}$: 43.8 (quaternary benzylic C), 41.8 (ArCCH_2), 30.4 (SiCH_2Cl), 17.8 ($\text{CH}_2\text{CH}_2\text{CH}_2$), 15.8 (SiCH_2CH_2), -4.2 (SiCH_3). The MALDI TOF mass spectrum shows the progressive loss of all the halogen atoms due to extensive fragmentations. Thus, MALDI TOF mass spectra of higher generation numbers were not recorded in the $G_n\text{-SiCH}_2\text{Cl}$ series, but with success for the polyallyl series (for a spectrum and the data, see Figure 3 and Table 1, respectively, and the Supporting Information).

Hydrosilylation of Higher-Generation G_n -Polyallyl. An identical procedure is used, and the reactions are monitored by ^1H and ^{29}Si NMR spectroscopy in order to reach completion (see text).

Second Reaction of the Dendritic Sequence: Nucleophilic Substitution of the Chloride by the Phenol Triallyl Dendron. Reaction of $G_0\text{-9-SiCH}_2\text{Cl}$ with the Dendron A. $G_0\text{-9-SiCH}_2\text{Cl}$ (0.500 g, 0.34 mmol), the dendron **A** (0.845 g, 3.70 mmol), K_2CO_3 (4.26 g, 30.9 mmol), and NaI (93 mg, 0.62 mmol) are introduced in a Schlenk tube under argon. Then, 50 mL of DMF is also transferred into the Schlenk tube via cannula, and the reaction mixture is stirred at 80 °C for 1 day. Then, the solvent is removed under vacuum, and the residue is dissolved in 20 mL of dichloromethane and filtered on Celite. This solution is washed with a $\text{Na}_2\text{S}_2\text{O}_3$ -saturated solution and dried over Na_2SO_4 . After filtration and reduction of the solvent volume under reduced pressure, excess methanol is added in order to precipitate the product. The gum obtained is dissolved in a minimum amount of dichloromethane and submitted to chromatography on a column of silica gel (eluent: dichloromethane). This yields 801 mg (73%) of $G_1\text{-27}$ (see formula in Scheme 1).

Reaction of Higher Generation $G_n\text{-SiCH}_2\text{Cl}$ with the Dendron A. The higher-generation polyallyl dendrimers are synthesized similarly (including the purification procedure), except that the reaction time is increased to 3 days. The ^1H and ^{29}Si NMR are shown in Figure 1 (the NMR spectra are similar for all the generations, following G_2). See the Supporting Information for the NMR spectra of all 10 generations. ^1H NMR (CDCl_3 , 400 MHz, δ_{ppm} vs TMS): 7.165 and 6.85 ($p\text{-C}_6\text{H}_4$, double d), 5.535 ($-\text{CH}=\text{CH}_2$, m), 4.96 ($-\text{CH}=\text{CH}_2$, m), 3.48 (SiCH_2 , s), 2.40 ($-\text{CH}_2-\text{CH}=\text{CH}_2$, d), 1.63 ($\text{CH}_2\text{CH}_2\text{CH}_2\text{Si}$, m), 1.14 ($\text{CH}_2\text{CH}_2\text{-CH}_2\text{Si}$, m), 0.57 ($\text{CH}_2\text{CH}_2\text{CH}_2\text{Si}$, m), 0.03 (SiMe_2 , s). The alkane impurity appears in the ^1H spectrum as shown in Figures 1 and 2 only as small signals. The intensity of the alkane signals can be diminished, but not suppressed, by successive reprecipitation from dichloromethane with methanol. ^{29}Si NMR (CDCl_3 , 59.62 MHz, δ_{ppm} vs TMS): 0.40 (SiCH_2O). Only one ^{29}Si NMR signal is observed for all the G_n -polyallyl dendrimers whatever the generation number. This indicates that the ^{29}Si NMR does not distinguish the Si atom layers of different generations and the same environment exists within a single dendrimer. Also, the inner layers contain comparatively too few Si atoms to be observed given the NMR accuracy, even if they have NMR shifts different from those of the outer layer. The completion of the nucleophilic substitution reaction is confirmed for each generation by the disappearance of the SiCH_2Cl signal near 3.8 ppm (this probe is all the more sensitive as this signal is larger than the SiCH_2O signal in the ^{29}Si NMR spectra of the G_n -poly- SiCH_2Cl compounds). ^{13}C NMR

(32) Lehn, J.-M. *Supramolecular Chemistry: Concepts and Perspectives*; VCH: Weinheim, 1995.

(33) For improved detailed experimental procedure, see: Astruc, D. In *Electron Transfer in Chemistry*; Balzani, V., Ed.; VCH-Wiley: New York, Vol. 2, 2001; Mattay, J., Astruc, D., Eds.; section 2: *Inorganic and Organometallic Compounds*, Chapter 4, pp 714–803.

(34) (a) This nucleophilic substitution was originally reported for $[\text{FeCp}(\eta^6\text{-C}_6\text{H}_5\text{Cl})][\text{BF}_4]$ in: Nesmeyanov, N. A.; Volkenau, N. A.; Isaeva, L. S.; Bolesova, I. N. *Dokl. Akad. Nauk SSSR*, **1967**, *176*, 106–108. (b) For a review of the CpFe^+ -induced nucleophilic aromatic substitution, see: Astruc, D. *Top. Curr. Chem.* **1991**, *160*, 47–95.

(35) Moulines, F.; Djakovitch, L.; Boese, R.; Gloaguen, B.; Thiel, W.; Fillaut, J.-L.; Delville, M.-H.; Astruc, D. *Angew. Chem., Int. Ed. Engl.* **1993**, *32*, 1075–1077.

(36) Lewis, L. N. *J. Am. Chem. Soc.* **1990**, *112*, 5998–6004.

(37) Schröder, M. *Chem. Rev.* **1980**, *80*, 187–227.

(CDCl₃, 100.6 MHz, δ_{ppm} vs TMS): 159.4 (SiCH₂OC_{Ar}), 145.6 (substituted arene core C), 137.2 (O-substituted arene C of the dendron), 134.7 (inner C=C), 127.4 (outer unsubstituted arene C of the dendron), 121.4 (unsubstituted arene core C), 117.4 (outer C=C), 113.5 (inner unsubstituted arene C of the dendron), 42.6 (benzylic quaternary C of the core and dendron), 42.0 (CH₂-CH=CH₂ and CH₂CH₂CH₂), 17.9 (CH₂CH₂CH₂), 14.6 (CH₂CH₂CH₂), 4.38 (SiCH₃). The arene cores C are no longer observed for higher generations. MALDI TOF mass spectrum: MNa⁺ ion at *m/z* 3 208, which corresponds to the molecular peak for M = 3 185 (no other peak).

Halogen Exchange by Reaction of G_n-Poly-SiCH₂Cl with NaI.

Example of G₀-9-SiCH₂Cl. G₀-9-SiCH₂Cl (0.240 g, 0.165 mmol), NaI (0.445 g, 2.96 mmol), and 50 mL of butanone are introduced under argon in a Schlenk tube. The reaction mixture is stirred at 80 °C for 1 day, then the solvent is removed under vacuum, the residue is dissolved in minimum ether, and this solution is washed with a saturated aqueous solution of Na₂S₂O₃. This ether solution is dried with Na₂SO₄ and filtered and the solvent is removed under vacuum, which yields 0.256 g (68%) of G₀-9-SiCH₂I. ¹H NMR (CDCl₃, 400Mz, δ_{ppm} vs TMS): 6.97 (s, 3H, unsubstituted arene core CH), 1.98 (s, 18H, CH₂I), 1.64 (m, 18H, CH₂CH₂CH₂Si), 1.08 (m, 18H, CH₂CH₂CH₂Si), 0.64 (m, 18H, CH₂CH₂CH₂Si), 0.11 (s, 54H, SiCH₃). ¹³C NMR (CDCl₃, 100.6 MHz, δ_{ppm} vs TMS): 145.6 (substituted arene core CH), 121.5 (unsubstituted arene core CH), 43.8 (benzylic quaternary C), 41.9 (CH₂CH₂CH₂Si), 17.8 (CH₂CH₂CH₂Si), 15.8 (CH₂CH₂CH₂Si), -2.6 (SiCH₃), -12.8 (CH₂I). ²⁹Si NMR (CDCl₃, 59.6 MHz, δ_{ppm} vs TMS): 4.9 (SiCH₂I).

Exchange of Chloro by Iodo for Higher Generations. The same procedure is used except that the reaction time is increased from 1 day at 80 °C for G₀-9-SiCH₂I to 2 days at 80 °C for G₉-177 047-SiCH₂I. The reactions are monitored by ¹H, ¹³C, and ²⁹Si NMR in order to reach completion. The heavy iodo atoms around G₉-177 407-SiCH₂I (see Figure 7) allow inter alia to record HRTEM pictures, whereas such pictures are not visible for the polychloro- and polyallyl dendrimers.

AFM Experiments. AFM samples were prepared by spin-coating of a suitable solution (adjusted on trial-error basis) of dendrimer in benzene. The freshly cleaved, highly oriented pyrolytic graphite (HOPG) was covered with the solution and spinned at 1000 rpm with subsequent 10–15 s extra spinning at 3000 rpm for complete drying in air. The AFM system was a Thermomicroscope CP Research capable of

measurements in multiple modes, and the sample imaging was done in air immediately after spin-coating. The noncontact or NC dynamic mode was used giving the weakest interaction with the surface and therefore the less chance of alteration. The cantilever/tip systems used were either Ultralever or Nanosensors, with typical tip (silicon tip) radius of curvature of 10 nm. The amplitude and phase imaging of this mode were used. The calibration in the vertical *z* direction was achieved by measuring a single step (3.35 Å) between two adjacent atomic planes of HOPG. A sample was considered as good when a monolayer of dendrimer or two (high generations) was measured by AFM. In the images the surface of HOPG was easily recognized by detecting the single steps of HOPG and by looking at the phase value of the naked HOPG surface, which was significantly contrasting with that of the HOPG covered with one monolayer of dendrimer. Therefore, monolayer dendrimers covering HOPG were easily recognized, and by playing with dilution, it was possible to go from isolated holes in the monolayer case to an isolated islands case. On some samples, successive repeated scanning of the same area could alter the shape of the submonolayer by tip-induced displacement of dendrimer molecules inducing also a transition from mono- to multilayers.

Acknowledgment. This article is dedicated to Professor Henri Bouas-Laurent, a distinguished colleague and friend, at the occasion of his 70th birthday. Assistance from Michel Petraud (NMR, CESAMO) and Michel Chambon (HRTEM) at the University Bordeaux I and financial support from the Institut Universitaire de France (D.A., IUF), the CNRS, and the Universities Bordeaux I and Paris VI are gratefully acknowledged.

Supporting Information Available: 400 MHz ¹H, 100.6 MHz ¹³C, and 59.6 MHz ²⁹Si NMR spectra for all generations (G₁ to G₉) of dendrimers, G₀-SiCH₂OH and ¹H NMR spectrum of a mixture of G₂-81-allyl and G₀-SiCH₂OH, and MALDI TOF mass spectrum of G₁-27-allyl. This material is available free of charge via the Internet at <http://pubs.acs.org>.

JA021147O